STEM CELLS TRANSLATIONAL MEDICINE

TISSUE ENGINEERING AND REGENERATIVE MEDICINE

A Comparative Translational Study: The Combined Use of Enhanced Stromal Vascular Fraction and Platelet-Rich Plasma Improves Fat Grafting Maintenance in Breast Reconstruction

PIETRO GENTILE,[a] AUGUSTO ORLANDI,[b] MARIA GIOVANNA SCIOLI,[b] CAMILLA DI PASQUALI,[a] ILARIA BOCCHINI,[a] CRISTIANO BENIAMINO CURCIO,[a] MICOL FLORIS,[a] VALERIA FIASCHETTI,[c] ROBERTO FLORIS,[c] VALERIO CERVELLI[a]

Key Words. Adipose • Adult stem cells • Autologous stem cell transplantation • Clinical translation • Stem cell transplantation • Tissue-specific stem cells

[a]Plastic and Reconstructive Surgery Department, [b]Institute of Anatomic Pathology, and [c]Department of Diagnostic Imaging, University of Rome Tor Vergata, Rome, Italy

Correspondence: Pietro Gentile, M.D., San Salvatore in Lauro Place, no. 15, 00186 Rome, Italy. Telephone: 393388515479; e-mail: pietrogentile2004@libero.it

Received January 3, 2012; accepted for publication March 5, 2012; first published online in SCTM *EXPRESS* April 13, 2012.

1066-5099/2012/$20.00/0

http://dx.doi.org/10.5966/sctm.2011-0065

ABSTRACT

The use of autologous fat grafting is ideal in breast reconstruction. However, published data on long-term outcomes and instrumental results of fat grafting to the breast are lacking. The purpose of this study was to review the authors' experience of fat grafting, evaluating the effects related to the use of enhanced stromal vascular fraction (e-SVF) and fat grafting with platelet-rich plasma (PRP) in the maintenance of fat volume in breast reconstruction, comparing the results with a control group. Twenty-three patients aged 19–60 years affected by breast soft tissue defects were analyzed at the Plastic and Reconstructive Department of the University of Rome Tor Vergata. Ten patients were treated with SVF-enhanced autologous fat grafts, and 13 patients were treated with fat grafting + platelet-rich plasma. The patients in the control group ($n = 10$) were treated with centrifuged fat grafting injection according to Coleman's procedure. The patients treated with SVF-enhanced autologous fat grafts showed a 63% maintenance of the contour restoring and of three-dimensional volume after 1 year compared with the patients of the control group treated with centrifuged fat graft, who showed a 39% maintenance. In those patients who were treated with fat grafting and PRP, we observed a 69% maintenance of contour restoring and of three-dimensional volume after 1 year. As reported, the use of either e-SVF or PRP mixed with fat grafting produced an improvement in maintenance of breast volume in patients affected by breast soft tissue defect. STEM CELLS TRANSLATIONAL MEDICINE *2012;1:341–351*

INTRODUCTION

The popularization of fat grafting is the result of an increased demand for breast augmentation with stromal vascular fraction (SVF) enhanced autologous fat graft. The immediate gratification and the absence of breast implants have become powerful motivators that have enticed patients to request this regenerative surgery.

During the last 5 years, an increasing number of publications have reported on this topic. The areas in which stromal vascular fraction cells have been used include radiotherapy-based tissue damage after mastectomy [1], breast augmentation [2], postmastectomy breast reconstruction [3], breast implant complications [4], calvarial defects [5], Crohn's fistulas and complex perianal fistula [6–9], damaged skeletal muscle [10], Parry-Romberg disease and facial lipoatrophy [11], scarring, gluteal soft tissue defect, pectus excavatus, dermatofibrosis [12], and vocal fold augmentation [13, 14].

Visceral and subcutaneous adipose tissue has been demonstrated to contain progenitor cells able to differentiate in multiple cell lineages [10, 15]. After centrifugation of collagenase-digested adult adipose tissue, a heterogeneous cell population named stromal-vascular fraction is obtained [15, 16]. This population contains adult stem cells named adipose-derived stromal cells (ASCs) [17]. ASCs might improve tissue outcomes by increasing vascularity and through the secretion of growth factors that improve tissue survival. Recently, the authors published works on the use of fat grafting in the lipostructure technique as described by Coleman (purified fat obtained after centrifugation at 3,000 rpm for 3 minutes) [18, 19] mixed with platelet-rich plasma (PRP) in plastic surgery [20], in lower chronic extremity ulcers [21], and in hemifacial atrophy [22]. Now, we present out experience using regenerative surgery with the SVF-enhanced autologous fat grafting in breast reconstruction. In

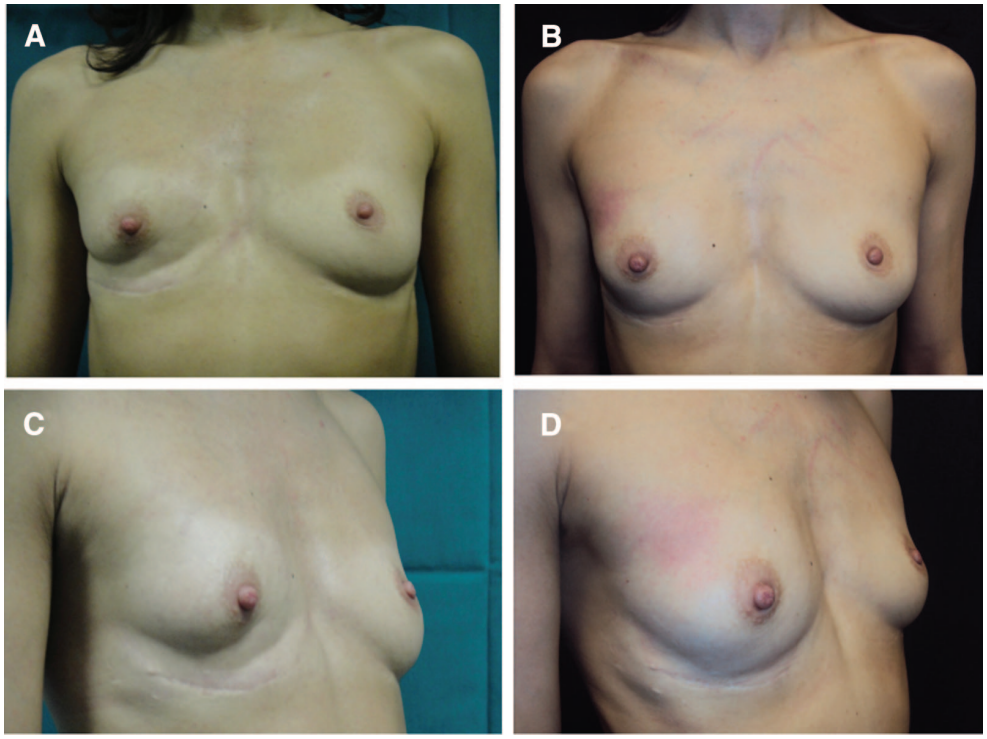

Figure 1. Breast reconstruction with fat graft + platelet-rich plasma. **(A):** Preoperative in frontal projection. **(B):** Postoperative in frontal projection after 1 year. **(C):** Preoperative in ¾ right projection. **(D):** Postoperative in ¾ right projection after 1 year.

this report, we present our studies using either SVF or PRP mixed with fat grafting and patient self-assessment of the outcomes as an additional parameter supporting the results of clinical assessment.

Materials and Methods

Patients

A total of 23 patients aged 19–60 years were treated from January 2008 to February 2012 at the Department of Plastic and Reconstructive Surgery of the University of Rome Tor Vergata.

Thirteen patients affected by breast soft tissue defects (3 patients affected by unilateral breast hypoplasia, 8 patients affected by outcomes of breast cancer reconstruction, and 2 patients after prosthesis removal) were treated with fat graft + PRP (supplemental online Table 1) for breast reconstruction (Fig. 1A, 1C). The purified fat was obtained after centrifugation at 3,000 rpm and placed in 1-ml syringes, and it was then aseptically reinserted using specific microcannulas for implanting. The 1 ml of centrifuged fat tissue was also mixed with 0.4 ml of PRP. The selection of location destined to receive the implant was determined taking into account the diversity in the lesions. To implant the fat tissue, small tunnels were previously created forcing the cannulas of 1.5 mm diameter with accurate and controlled movements. Once the fat tissue had been implanted at different levels, the access incisions were closed using 5-0 nylon stitches, and no compressive bandage was applied.

Ten patients (2 patients affected by unilateral breast hypoplasia, 7 patients affected by outcomes of breast cancer reconstruction, and 1 patient after prosthesis removal) were treated with SVF-enhanced autologous fat grafts (supplemental online Table 2), obtained using the Celution System (Fig. 2A). The patients were subjected to additional wash and centrifugation cycles, after which 5 ml of the enhanced SVF (e-SVF) suspension was extracted from the system. The e-SVF (5 ml) was added to the tissue collection container with the liposuction. Subsequent to the carrying out of a washing step, the e-SVF suspension was added and mixed with the washed fat graft. Using specific microcannulas for implantation, the SVF-enhanced fat graft was transferred into 10-ml syringes and aseptically reinjected into the soft tissue defect. The preoperative evaluation included a complete clinical examination, a photographic assessment, nuclear magnetic resonance imaging (MRI) (Fig. 3A, 3B) of the soft tissue, and ultrasound. In addition, in the more complex cases, such as the case with absence of pectoralis muscle and Poland syndrome, a high-resolution computed tomography scan with three-dimensional imaging was performed. Postoperative follow-up took place at 2, 7, 15, 21, and 36 weeks and then annually.

To establish the effects of their treatment, we compared our results with a control group made up of 10 patients (supplemental online Table 3). The control group comprised 10 females aged 21–65 years, all affected by breast soft tissue defects (3 patients affected by unilateral breast hypoplasia, 5 patients affected by outcomes of breast cancer reconstruction, and 2 patients after prosthesis removal). This sample group was treated with centrifuged fat grafting injection according to the Coleman procedure.

Exclusion criteria were divided into two types: local and systemic. The systemic criteria include platelet disorders, thrombocytopenia, antiaggregating therapy, bone marrow aplasia, uncompensated diabetes, sepsis, and cancer. The local criteria include cancer loss of substance. We did not use tobacco use or genetic disorders as exclusion criteria. This study is part of a

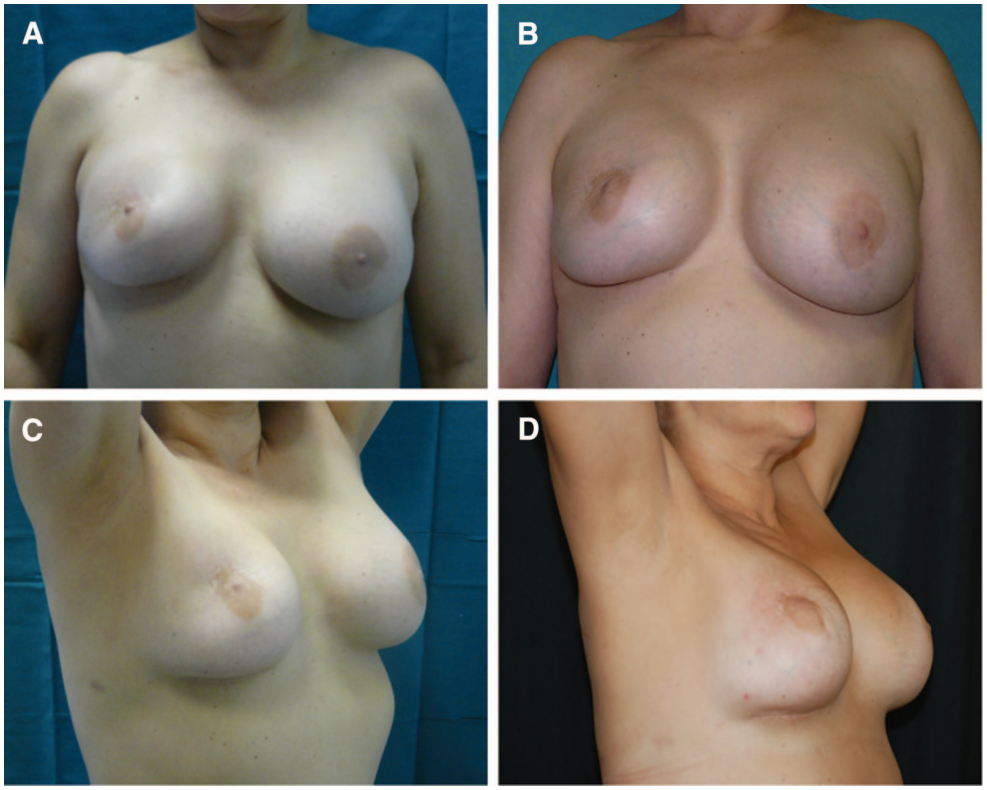

Figure 2. Patients treated with stromal vascular fraction-enhanced autologous fat grafts. **(A):** Preoperative in frontal projection. **(B):** Postoperative in frontal projection after 1 year. **(C):** Preoperative in ¾ right projection. **(D):** Postoperative in ¾ right projection after 1 year.

research project approved by Tor Vergata, and all procedures were performed under written patient informed consent and according to the guidelines of the local committee on human research.

Harvest Region and Preparation of the SVF-Enhanced Autologous Fat Graft

The cell and tissue preparation procedure mainly exhibited two phases. Phase 1 started with a syringe liposuction (715.4 ml average in all patients; range, 250–1,080 ml) in the abdominal region using 3-mm cannulas (supplemental online Fig. 1A). While aseptic technique was maintained, the plunger of the 60-ml syringe was removed, and the tip was closed with a cap. Half of the lipoaspirate (234.46 ml average) was placed into the tissue collection container of the Celution 800/CRS System (Cytori Therapeutics Inc., San Diego, http://www.cytoritx.com) (supplemental online Fig. 1B). Blood and free lipid was removed from the tissue (supplemental online Fig. 1D) through a wash cycle (supplemental online Fig. 1C), and the Celase 835/CRS Reagent (Cytori Therapeutics) was added to enzymatically digest the tissue, which released SVF (supplemental online Fig. 1E). After additional wash (supplemental online Fig. 1F) and centrifugation cycles (supplemental online Fig. 1G), 4–5 ml of the SVF suspension was extracted from the system (supplemental online Fig. 1H). In the second phase, the remaining part of the lipoaspirate was added to the tissue collection container (supplemental online Fig. 2A) and a washing step was automatically carried out (supplemental online Fig. 2B). Once completed, the 4–5 ml of SVF suspension was added (supplemental online Fig. 2C) and mixed with the washed fat graft (supplemental online Fig. 2D), resulting in approximately 429.61 ml (range, 60–620 ml) of SVF-enhanced fat tissue for grafting (supplemental online Fig. 2E). This newly processed cell-enhanced fat graft typically consists of 25%–30% water, which will be reabsorbed by the body in the postoperative period. This overall process was controlled through automated sensors and processing algorithms that ensured standard handling of the tissue and cells, and the process was completed within 160 minutes. The SVF-enhanced fat graft was transferred into 10-ml syringes (supplemental Fig. 2F) and aseptically reinjected into the patient using specific microcannulas for implantation (supplemental Fig. 2G, 2H).

The donor site region was infiltrated with a cold saline solution containing 1 ml of adrenaline per 500 ml of saline solution without lidocaine or carbocaine. Adipose tissue was removed after 5 minutes using a 3-mm-diameter cannula and a 60-ml Toomey syringe. We reinjected the SVF-enhanced adipose tissue using specific microcannulas (1–2 mm in diameter) for implantation.

Surgical Technique and Location of Implantation

The area destined to receive the graft was determined on the basis of the necessary corrections. Based on the necessary corrections, the harvested material was implanted for breast augmentation prevalently into three areas: inferior breast rim, superior and inferior regions of the areola, and the superior lateral quadrant.

After pretunnelling, fat tissue was implanted (395.4 ml average [range, 80–600 ml]; 197.7 ml average for each breast) at different levels using a delivery cannula (1–2 mm in

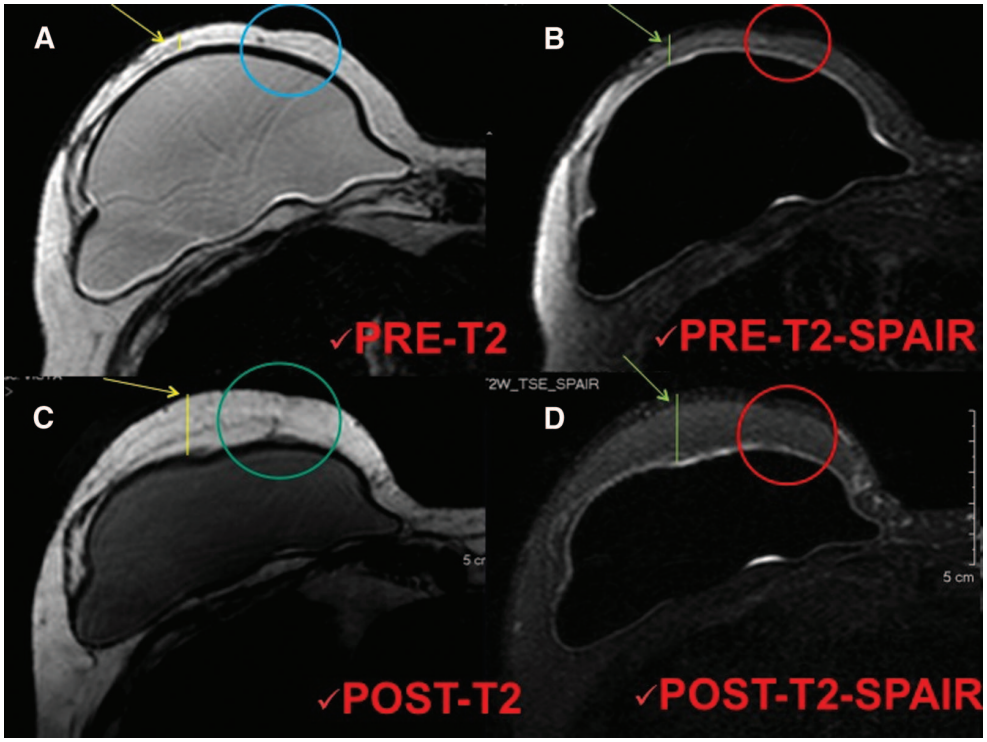

Figure 3. Magnetic resonance imaging of a patient treated with enhanced stromal vascular fraction fat grafting. **(A, B):** T2 imaging **(A)** and T2 SPAIR imaging **(B)** of the preoperative situation. Arrows show the critical point of the reduced thickness, the lines show the reduced thickness of the tissue, and the circles show the local soft tissue defect characterized by a loss of volume. **(C, D):** T2 imaging **(C)** and T2 SPAIR imaging **(D)** of the postoperative situation after 1 year. Arrows show the improvement of the critical point, the lines show the increased thickness of the tissue, and the circles show the correction of the local soft tissue defect with maintenance of volume. Abbreviation: SPAIR, spectral attenuated inversion recovery.

diameter) with precise, controlled movements. Small quantities of the SVF-enhanced fat graft were injected while the cannula was withdrawn, to create a large grid to increase survival of the transplanted tissue. Several layers were laid down to increase the contact surface between the receiving tissue and the implant; this technique is of fundamental importance to allow each layer deposited to survive by diffusion during the few days necessary for growth of blood vessels that will nourish the implant permanently [1, 2, 4, 6]. The incisions were closed with 5-0 nylon sutures, and no compressive bandage was applied.

Stromal Vascular Fraction Nucleated Cell Isolation and Counting

For manual SVF extraction, liposuction aspirates were washed three times with phosphate-buffered saline (PBS) and suspended in an equal volume of PBS and 0.1% collagenase type I (C130; Sigma-Aldrich, Milan, Italy, http://www.sigmaaldrich.com) prewarmed to 37°C. Adipose tissue was placed in a shaking water bath at 37°C with continuous agitation for 60 minutes and centrifuged for 10 minutes at 600*g* at room temperature. The supernatant, containing mature adipocytes, was aspirated. The SVF pellet was resuspended in erythrocyte lysis buffer (155 mM NH_4Cl, 10 mM $KHCO_3$, and 0.1 mM EDTA) and incubated for 5 minutes at room temperature. After centrifugation at 1,100 rpm for 5 minutes, the pellet was resuspended in few microliters of growth medium (Dulbecco's modified Eagle's medium [DMEM] supplemented with 10% fetal bovine serum [FBS], 2 mM L-glutamine, 100 U/ml penicillin, 100 μg/ml streptomycin, and 0.25 μg/ml amphotericin B [Fungizone; Invitrogen, Milan, Italy, http://www.invitrogen.com]) and passed through a 100-μm Falcon strainer (Becton, Dickinson and Company, Sunnyvale, CA, http://www.bd.com). Then, to evaluate SVF extraction, cellular suspension was counted by using a hemocytometer with trypan blue staining exclusion. Cell viability by trypan blue exclusion was consistently more than 98%.

PRP Preparation

The types of PRP preparation may be divided in two categories: manual methods and methods that rely on use of semiautomatic or automatic devices. Briefly, the process of preparing PRP consists of four phases: blood collection, centrifugation for platelet concentration, induction of gelation (if the PRP is used in the gel form), and activation.

The manual preparation of PRP consisted of a slow centrifugation, which allows the platelets to remain suspended in the plasma while the leukocytes and erythrocytes are displaced to the bottom of the tube. A rapid centrifugation can cause mechanical forces and elevate the temperature, thus inducing changes in the ultrastructure of platelets that, in turn, can initiate a partial activation, with a subsequent loss of their granular content [20]. The current systems for preparation of platelet concentrations routinely report the use of various centrifugation rates (we used a 1,100*g* centrifuge). After centrifugation, the buffy coat layer, consisting of platelets and white blood cells, was sequestered in a volume of 9 ml of plasma.

Standard cell separators and salvage devices can be used to produce platelet-rich plasma. These devices operate on a unit of blood and typically use continuous-flow centrifuge bowl or continuous-flow disk separation technology and both a hard (fast) and a soft (slow) spin, yielding platelet concentrations from two to four times baseline [23, 24]. Such devices include the CATS (Fresenius, Wilmington, DE), Sequestra (Medtronic, Minneapolis, MN, http://www.medtronic.com), Cell Saver 5 (Haemonetics Corp., Braintree, MA, http://www.haemonetics.com), and others [23–25]. Many surgical procedures require use of relatively small volumes of platelet-rich plasma [26]. Consequently, small, compact office systems have been developed that produce approximately 6 ml of platelet-rich plasma from 45–60 ml of blood [26, 27]. There are many such systems, including the GPS (Biomet, Warsaw, IN, http://www.biomet.com/), the PCCS (Implant Innovations, Inc., Palm Beach Gardens, FL, http://biomet3i.com), the Symphony II (DePuy, Warsaw, IN, http://www.depuy.com), the SmartPReP (Harvest Technologies Corp., Norwell, MA, http://www.harvesttech.com), and the Magellan (Medtronic) [23, 26, 27]. Although all operate on a small volume of drawn blood (45–60 ml) and on the principle of centrifugation, these systems differ widely in their ability to collect and concentrate platelets, with approximately 30%–85% of the available platelets collected and from a less than twofold to an approximately eightfold increase in the platelet concentration over baseline [23, 24].

There are several devices for the PRP preparation, such as Fibrinet (Cascade Medical Enterprises, Plymouth, U.K.), Regen (Regen Lab, Le Mont-sur-Lausanne, Switzerland, http://www.regenlab.com), Plateltex (Plateltex S.R.O., Bratislava, Slovakia, http://www.plateltex.com/), and Vivostat (Vivostat A/S, Alleroed, Denmark, http://www.vivostat.com). Generally, we prepared the PRP according to the Cascade method and in all cases under a protocol approved by our institution's transfusion service.

In general, most systems, whether large or small volume, do not concentrate the plasma proteins of the coagulation cascade [23, 25]. The concentration of plasma protein levels above baseline can be achieved through secondary ultrafiltration, as is done with the Ultra Concentrator (Interpore Cross, Irvine, CA), and the Access System (Interpore Cross), in which the buffy coat collected from a centrifugation stage is passed through hollow fibers with an effective pore size of 30 kDa. This system removes by filtration up to two-thirds of the aqueous phase; thus, the concentrations of the plasma proteins retained and the elements formed are increased substantially [28].

In our procedure, PRP was prepared in the presence of a transfusional service doctor from a small volume of blood (18 ml) according to the method of the Cascade-Esforax system [20] (supplemental online Fig. 3E), a commercially approved formulation. Briefly, to prepare PRP, blood was taken from a peripheral vein using sodium citrate as an anticoagulant. This system for preparing platelet concentrations uses centrifugation of 1,100*g* for 10 minutes (supplemental online Fig. 3E). The PRP protocol uses Ca^{2+} to induce platelet activation and exocytosis of the α granules. We added Ca^{2+} when the fat was centrifuged. The final aim was to obtain a platelet pellet (supplemental online Fig. 3F, 3G), although the preparation was not selective and included leukocytes. The secretion of growth factor begins with platelet activation.

Fat Graft Centrifugation According to the Coleman Procedure and Mix with PRP

Before proceeding to activation of PRP, under general anesthesia we harvested fat tissue from the abdominal region using some specific cannulas. Maintaining asepsis, we took the plungers off the syringes; after closing them with a cap, we positioned them flat in the sterile centrifuge (supplemental online Fig. 3A). The syringes were processed for 3 minutes at 3,000 rpm (supplemental online Fig. 3B). This procedure obtained purified fat tissue (supplemental online Fig. 3C), preserving the integrity of the adipocytes but separating the fluid fat portion from the serous-bloody part (supplemental online Fig. 3D). We mixed 0.5 ml of PRP with 1 ml of centrifuged fat tissue (supplemental online Fig. 3I, 3L). The purified body fat mixed with PRP was put in 1-ml syringes (supplemental online Fig. 3M, 3N) and aseptically reinserted using the specific microcannulas for implanting.

Clinical Evaluation Method

Two methods for the clinical evaluation of outcomes were used: (a) team evaluation, and (b) patient self-evaluation. The team evaluation is an evaluation method based on clinical observation, using a scale of six values (excellent, good, discreet enough, poor, inadequate). The patient-based self-evaluation uses the same six values mentioned above. The factors/variables that were taken into account were pigmentation, vascularization, pliability, thickness, itching, and pain.

The percentage of maintenance restored was clinically evaluated with two different criteria. The first was the subjective evaluation, and the second one was the objective evaluation. The subjective evaluation was based on the personal score of each patient focused on the following parameters: (a) presence of asymmetry, deformity, irregularity, dyschromia, dysesthesia, paraesthesia, and pain; (b) results of the supero-external quadrant, infero-external quadrant, supero-internal quadrant, and infero-internal quadrant; (c) resorption of fat in one or more regions; (d) time of stabilization of the transplanted fat; and (e) need for retreatment.

For each parameter, patients gave a yes/no or positive/negative evaluation, and percentage of maintenance of restored was calculated as the mean of all calculated single percentages. The objective evaluation was made on the analysis of the preoperative and postoperative photos. The photos were of the same size, brightness, and even contrast. According to parameters reported above, the operator similarly calculated the percentage of restoration. Finally, the mean between patient and operator evaluations was calculated.

Instrumental Imaging Evaluation Method

The percentage of maintenance restored was imaging evaluated with MRI (Figs. 3, 4). The timing was as follows: preoperative (Fig. 3A, 3B), after 6 and 12 months (Fig. 3C, 3D), and then annually.

MRI showed that transplanted fat tissue survived and formed a significant thickness of the fatty layer not only subcutaneously on and around the mammary glands but also between the mammary glands and the pectoralis muscles. Although small cystic formation and macrocalcification were detected in one case, the macrocalcification was easily distinguished from that associated with breast cancer, and the overall cosmetic results were generally satisfactory and encouraging. Almost all the patients were satisfied with their enlarged and soft breasts with a natural contour.

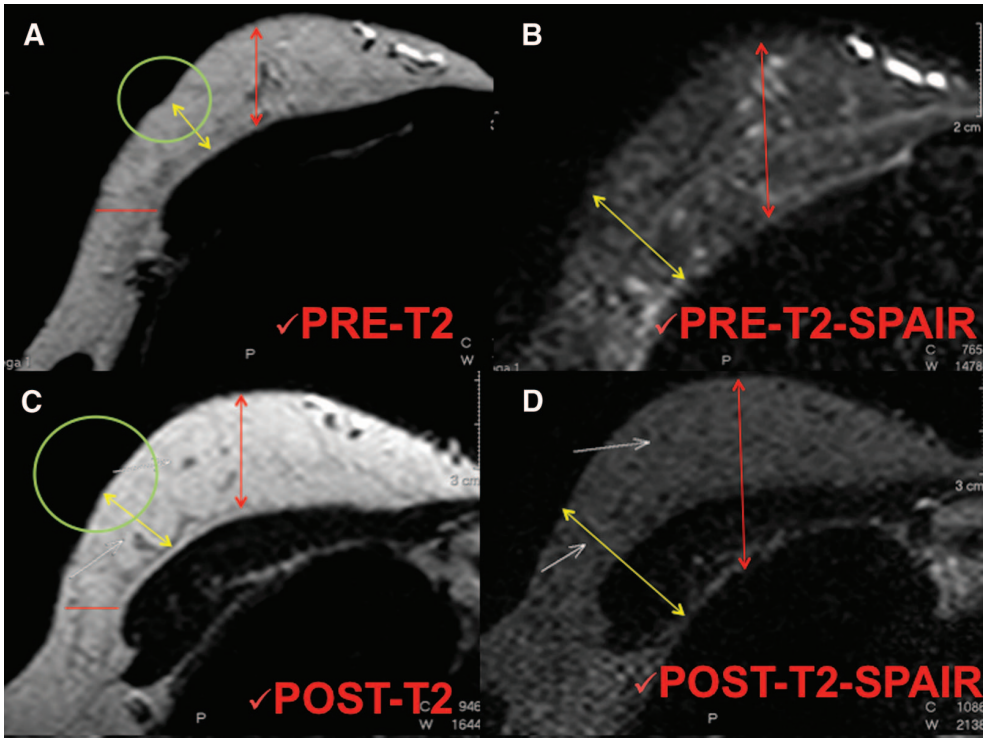

Figure 4. Magnetic resonance imaging of a patient treated with fat grafting mixed with platelet-rich plasma. **(A, B):** T2 imaging **(A)** and T2 SPAIR imaging **(B)** of the preoperative situation. Circles show the critical point of the reduced thickness, the yellow arrows show the reduced thickness of the tissue in the critical point, and the red arrows show the normal soft tissue thickness near the defect. **(C, D):** T2 imaging **(C)** and T2 SPAIR imaging **(D)** of the postoperative situation after 1 year. Circles show the absence of the critical point with a completely correction of the defect, yellow arrows show the increased thickness of the tissue and maintenance of fat volume in the critical point, and red arrows show the augmentation of soft tissue volume. Abbreviation: SPAIR, spectral attenuated inversion recovery.

ASC Differentiation Potential and Growth Curves

To demonstrate the differentiation capacity of cultured ASCs, adipogenic (Fig. 5A, 5B) and osteogenic (Fig. 5C, 5D) differentiation was verified in third-passage confluent cells, according to previously published methods [20]. Briefly, for adipogenesis, ASCs were cultured in DMEM supplemented with 10% FBS, 100 μM L-ascorbic acid, 1 μM dexamethasone, 0.5 mM 1-methyl-3-iso-butylxanthine, 100 μM indomethacin, and 10 μg/ml human recombinant insulin (Sigma-Aldrich). Control was cultured in DMEM plus 10% FBS. Medium was changed every 3 days for 3 weeks, and adipogenesis was assessed by Oil Red O staining. Osteogenic differentiation was induced in DMEM supplemented with 10% FBS, 200 μM L-ascorbic acid, 0.1 μM dexamethasone, and 10 mM β-glycerol phosphate (Sigma-Aldrich). Control was cultured in DMEM plus 10% FBS. Medium was changed every 3 days for 21 days. To assess mineralization corresponding to osteogenic differentiation, intracellular calcium deposits were stained with von Kossa stain (Fig. 5C, 5D). Images were obtained at a magnification of $\times$200 through a digital camera (Dxm1200F; Nikon, New York, http://www.nikon.com) connected to a computer using Nikon ACT-1 software. For growth curves (Fig. 5G), third-passage ASCs were seeded at 2,500 cells per cm^2, serum starved overnight, and maintained in DMEM plus 10% FBS (control) or DMEM + 10% FBS + PRP (5% vol/vol) for 6 days. Every 2 days, cells were trypsinized and counted using a hemocytometer. In some experiments, epidermal growth factor receptor (EGFR) and ErbB2 selective inhibitors were used at 5 μM (AG1478 and AG879; Sigma-Aldrich). The inhibition of ASC proliferation was expressed as the percentage of reduction compared with PRP-control (mean $\pm$ SE). Each experiment was performed in triplicate.

Immunofluorescence

Control and PRP-treated ASCs (after 6 days of treatment) were fixed in 4% paraformaldehyde for 5 minutes at 4°C and then incubated with mouse monoclonal antibody anti-CD44 and anti-CD90 (Santa Cruz Biotechnology Inc., Santa Cruz, CA, http://www.scbt.com) for 1 hour at room temperature. Anti-mouse secondary antibody (Nordic Immunological Laboratories, Tilburg, The Netherlands, http://www.nordiclabs.nl) was added, and then cells were incubated with fluorescent streptavidin (R&D Systems Inc., Minneapolis, http://www.rndsystems.com). Hoechst was used for nuclear staining.

Western Blot Analysis

After extraction and quantification of total cell lysates, proteins were separated by gradient sodium dodecyl sulfate-polyacrylamide gel electrophoresis, blotted to nitrocellulose transfer membranes, and incubated with anti-CD44 (Santa Cruz Biotechnology), anti-CD90 (Santa Cruz Biotechnology), anti-EGFR (Cell Signaling Technology, Beverly, MA, http://www.cellsignal.com), anti-c-erbB-2 (Upstate, Charlottesville, VA, http://www.upstate.com; Millipore, Billerica, MA, http://www.millipore.com), anti-phosphorylated ErbB2 (pTyr1248) (Sigma-Aldrich), and anti-α-tubulin antibody (Sigma-Aldrich). Each experiment was performed in triplicate.

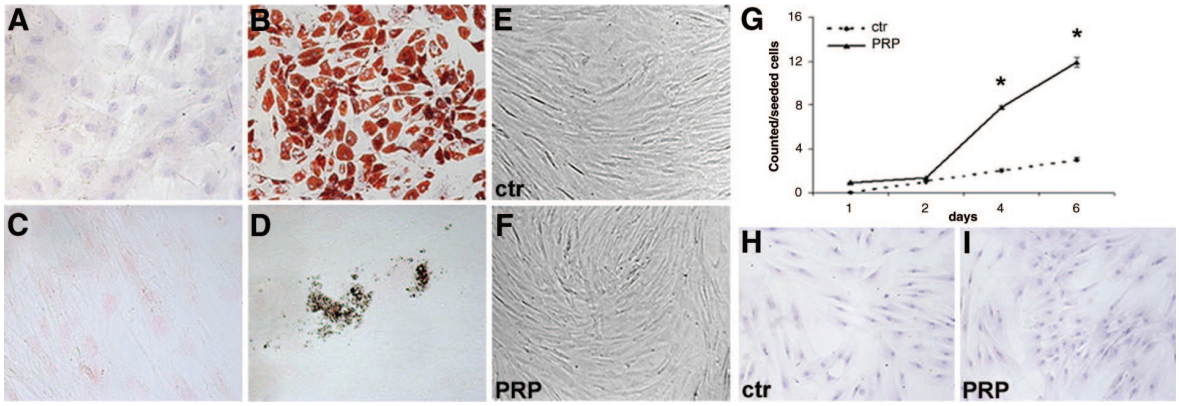

Figure 5. Adipogenic and osteogenic differentiation of adipose-tissue-derived stem cells (ASCs). **(A, B):** Oil Red O staining of control ASCs (Dulbecco's modified Eagle's medium [DMEM] + 10% fetal bovine serum [FBS]) **(A)** and ASCs after induction of adipocyte differentiation **(B)**. **(C, D):** Nuclei were counterstained with hematoxylin and von Kossa staining in control ASCs (Dulbecco's modified Eagle's medium [DMEM] plus 10% fetal bovine serum [FBS]) **(C)** and ASCs after induction of osteogenic differentiation **(D)**. Nuclei were counterstained with Fast Red. **(E, F):** Contrast phase micrographs showing the similar morphological appearance of control and PRP-treated cells. Magnification, ×100. **(G):** Growth curve of control (DMEM + 10% FBS) and PRP-treated ASCs (DMEM + 10% FBS + 5% PRP) showing an increase of cell number with PRP treatment (∗, $p < .02$; *t* test). **(H, I):** Oil Red O staining of control and PRP-treated ASCs showing a similar intracytoplasmic accumulation of small lipid droplets in both groups. Magnification, ×100. Abbreviations: ctr, control; PRP, platelet-rich plasma.

Statistical Analysis

Values as mean plus SE were analyzed by means of Student's *t* test, and differences considered statistically significant at $p < .05$. For three or more groups of univariate data, single-factor analysis of variation was used to obtain *p* values.

RESULTS

Patients treated with SVF-enhanced autologous fat grafts (Fig. 2B) showed a 63% maintenance of contour restoring and three-dimensional volume after 1 year (Fig. 6, red column) compared with 39% for the control group treated with centrifuged fat graft ($p < .0001$; Fig. 6, green column). In patients treated with reconstructing three-dimensional projection of breast by fat grafting and PRP (Fig. 1B, 1D), we observed a 69% maintenance of contour restoring and three-dimensional volume after 1 year ($p < .0001$ vs. control group; Fig. 6, blue column).

Transplanted fat tissue resorption was analyzed with instrumental MRI as suggested by Salgarello et al. [29] and ultrasound. Compared with breast reconstruction using autologous centrifuged fat, reconstruction with SVF-enhanced fat tissue (Fig. 2B, 2D) and fat graft + PRP (Fig. 1B, 1D) showed a smaller rate of fat resorption.

Compared with breast reconstruction using implants of the same size, augmentation with SVF-enhanced fat tissue showed a lower height but a more natural contour and softness of the breasts. All the patients were satisfied with the resulting texture, softness, and contour, and MRI confirmed the maintenance of restoration (Figs. 3, 4). As reported, e-SVF and PRP mixed with fat grafting demonstrated an improvement in maintenance of breast volume in patients affected by breast soft tissue defect.

Stromal Vascular Fraction Nucleated Cells from Automatic and Manual Extraction

As previously published [30], from adipose tissue, by manual extraction, we obtained approximately 250,000 ± 34,782 nucleated cells per milliliter of fat tissue. Using the automatic extractor, however, cell yield was approximately 50,000 ± 6,956 nucleated cells per milliliter of fat tissue ($p < .01$).

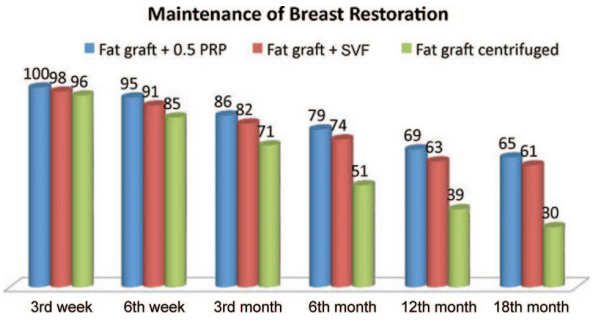

Figure 6. Clinical evaluation of fat graft volume maintenance in breast restoration. Abbreviations: PRP, platelet-rich plasma; SVF, stromal vascular fraction.

PRP Increases Adipose Tissue Stem Cell Number In Vitro

As we reported previously [20], PRP induced an increase of ASC number (Fig. 5G) compared with 10% serum control without any morphological changes (Fig. 5E, 5F). There was a statistically significant increase of cell number with PRP treatment, approximately fourfold, at days 4 and 6, when cells were preconfluent ($p < .02$). In addition, Oil Red O staining did not reveal any significant difference in intracytoplasmic lipid accumulation compared with PRP-treated and control ASCs (Fig. 5H, 5I). Immunofluorescence and Western blot analysis for stromal markers CD44 and CD90 did not show differences between control and PRP-treated ASC immunophenotype (Fig. 7).

How Does PRP Improve ASC Proliferation?

We investigated the effects of PRP in proliferation of ASCs: we first investigated ErbB receptor expression. EGFR and other members of the ErbB tyrosine kinase receptor family regulate several cell biology processes, including proliferation, survival, differentiation, and tumorigenesis [31, 32]. We observed that serum-cultured ASCs expressed lower EGFR and ErbB2 transcript levels compared with adult subcutaneous adipose tissue (not

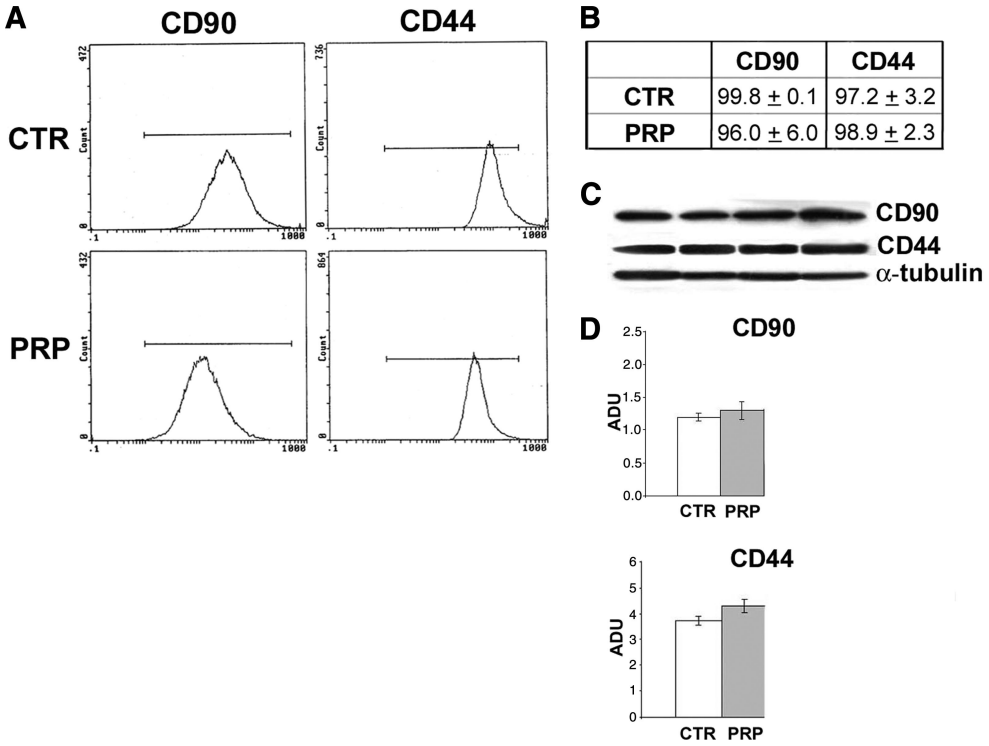

Figure 7. Effect of platelet-rich plasma on stromal marker expression in human adipose-derived stem cells. **(A, B):** Flow cytometry **(A)** and percentages of stromal markers CD90 and CD44 positivity **(B)** in serum control PRP (5% vol/vol) for 6 days. **(C):** Blot analysis of CD90 and CD44 protein in serum control PRP (5% vol/vol) for 6 days. **(D):** Densitometric analysis of CD90 and CD44 protein expression after blotting. Abbreviations: ADU, arbitrary densitometric units; CTR, control; PRP, platelet-rich plasma.

shown). Western blot documented that PRP, after 6 days of treatment, induced the downregulation of EGFR (43.2 ± 5.7% reduction compared with serum control; $p < .05$) and the marked downregulation of ErbB2 activity (82.3 ± 7.8% reduction compared with serum control; $p < .01$). To confirm the role of EGFR and ErbB2 in the control of ASC proliferation, we used the specific inhibitors AG1478 and AG879, respectively. Both these inhibitors reduced ASC proliferation (50.2 ± 9.3% and 49.5 ± 8.9% reduction compared with PRP alone, respectively; $p < .01$).

In addition, real-time polymerase chain reaction documented that after 6 days of combined PRP-insulin treatment of ASC adipogenic differentiation was significantly associated with an increase in fibroblast growth factor receptor (FGFR)-2 transcript level and less significantly with an increase in FGFR-1 transcript level ($p < .01$ and $p < .05$ vs. control, respectively); FGFR-2 mRNA upregulation was already evident after 12 hours. The selective FGFR-1 inhibitor PD166866 reduced cell number and intracytoplasmic lipid accumulation (approximately 30%) in PRP + insulin-treated compared with control ASCs ($p < .05$ and $p < .001$, respectively). A similar reduction of cell number and lipid accumulation was observed with the total FGFR inhibitor PD173074, strongly suggesting that the inhibition of FGFR-2 activity affects ASC adipogenesis and proliferation minimally or not at all. Instead, insulin-like growth factor (IGF) receptor selective inhibition did not modify ASC lipid accumulation and in combination did not amplify FGFR inhibitor effects. Finally, PD166866 inhibitor markedly inhibited Akt phosphorylation in control and in combined PRP + insulin-treated ASCs ($p < .001$ and $p < .01$, respectively). Similar effects were observed with PD173074 (data not shown). These findings support the crucial role of FGFR-1 signaling in Akt-dependent adipogenic commitment of ASCs.

Moreover, Giacco et al. [33] tested the effect of specific tyrosine kinase receptor inhibitors (tyrphostins) on thrombin-activated platelet (TAP)-induced tyrosine phosphorylation and cell growth. A platelet-derived growth factor receptor (PDGF-R) inhibitor, AG1296 (10 μM), reduced the PDGF-R 185-kDa and the IGF-1 receptor (IGF-1-R) β-subunit 95-kDa species by 70% and 50%, respectively. At variance with this, AG1024 (10 μM), an IGF-1-R inhibitor, selectively decreased IGF-1-R β-subunit tyrosine phosphorylation [33]. The identity of the bands was confirmed by immunoblot with PDGF-R and IGF-1-R β-subunit antibodies. In addition, AG1296 and AG1024 reduced thymidine incorporation by 50% and 60%, respectively. By contrast, no effect was achieved when the cells were pretreated with 10 μM SU1498 (a vascular endothelial growth factor [VEGF] receptor inhibitor). In conclusion, the PDGF-R blocker Ag1296 reduced the activation of Akt/PKB and, to a lesser extent, of ERK1/2. Conversely, inhibition of IGF-1 signaling by Ag1024 and expression of a dominant-negative IGF-1-R mutant selectively reduced the stimulation of ERK1/2 by TAPs and fibroblast-released factors, with minor changes in Akt/PKB activity [33].

Discussion

In this case series, supplementation of autologous fat grafts using SVF improved breast soft tissue defects compared with fat

grafting alone. Although small cystic formation and microcalcification were detected in one case, the microcalcification was easily distinguished, by checking with ultrasound, from that associated with breast cancer, and the overall cosmetic results were generally satisfactory and encouraging. In this case, we did not perform a biopsy because the clinical features and ultrasound images of the microcalcification confirmed the diagnosis of fat necrosis-associated microcalcification.

Lipofilling procedures can modify radiologic images; however, this interference has been studied in the literature [34–36], and radiologic studies suggest that imaging technologies (ultrasound, mammography, and MRI) can identify the microcalcifications caused by fat injection [37]. Moreover, recent follow-up studies have demonstrated the safety of the procedure, detecting no increase in new disease or tumor recurrence [3, 34, 38]. Almost all the patients were satisfied with their enlarged and soft breasts with a natural contour. MRI showed that transplanted fat tissue survived and formed a significant thickness of the fatty layer not only subcutaneously on and around the mammary glands but also between the mammary glands and the pectoralis muscles. Maximum breast augmentation using the technique described varied among the patients and appeared to be 80–180 ml. Although these volumes may be smaller than those achieved with large artificial implants, a definite advantage is that patients need not be concerned about postoperative complications induced by artificial implants, such as rupture, infection, capsular contracture, unnatural contour, hardness, neurologic symptoms, and immune response. Compared with patients who underwent conventional autologous fat graft to the breasts, augmentation effects were apparently higher with SVF-enhanced fat.

For each injection, a 0.5–1.2-cm increase in breast soft tissue volume was common with the conventional procedure, compared with the 1.2–2.8-cm increase seen in this trial of SVF-enhanced fat, although the augmentation effect varied among patients. The measurement system we recently devised may help to quantify the difference in augmented volume in the future.

The potential benefit of SVF supplementation could be explained by the ability of cells to secrete various growth factors that improve survival and increased vascularization [18, 22], leading to increased survival of the graft as shown a rodent study [19]. In light of this concept, we propose the chain of events leading to regeneration of the tissue to be as follows: targeting of damaged areas, release of angiogenic and antiapoptotic factors, and then formation of new vessels and oxygenation.

SVFs might indeed improve fat graft survival and maintenance, which is supported by observations from other surgical procedures, such as maxillofacial surgery for a calvarial defect [2] and breast reconstruction after partial mastectomy with radiotherapy damage [39]. Implanted adipose tissue must survive by a simple diffusion mechanism until an active blood supply is reestablished. Thus survival of the graft, particularly of a larger volume graft, is balanced between this process and hypoxia-induced cell death [40]. Prosurvival factors may therefore promote long-term retention and hence durability of the graft. In an animal study, this effect was achieved by using gene therapy to deliver VEGF (a potent proangiogenic factor) to the graft. This resulted in increased blood vessel density within the graft and a significant improvement in graft retention at 15 weeks [41].

The traditional preparation of growth factors contained in PRP consisted of a slow centrifugation, which allows the platelets to remain suspended in the plasma while the leukocytes and erythrocytes are displaced to the bottom of the tube. The current systems for preparing platelet concentrations use various centrifuges. The final aim was to obtain a platelet pellet, although the preparation is not selective and includes leukocytes. The secretion of growth factor begins with platelet activation. The PRP protocol uses Ca^{2+} to induce platelet activation and exocytosis of the α granules. A rapid centrifugation can cause mechanical forces and can raise the temperature, thus inducing changes in the ultrastructure of platelets that, in turn, can initiate a partial activation, with a consequent loss of its content [20].

Calcium acts as a necessary cofactor for platelet aggregation [20]. When Ca^{2+} is used to induce platelet activation, the secretion of the growth factors contained in the granules is slow [20]. To optimize the secretion process, the optimum concentration of Ca2 was previously determined [20]. When a rapid activation and coagulation is required, endogenous thrombin could be used.

Anitua et al. [42] reported the use of two centrifugation rates. Blood was collected into 3.8% (wt/vol) sodium citrate and centrifuged at 4,500*g* for 12 minutes at 4°C to obtain platelet-poor (PP) plasma or at 460*g* for 8 minutes to obtain PRP. Calcium chloride was added to PP and PRP at a final concentration of 22.8 mM. The secretion of growth factor begins with platelet activation.

In an interesting work, Mazzucco et al. described the different growth factor concentrations that are obtained through different devices (Fibrinet, Plateltex, and Regen) and a homemade method [43]. PDGF-BB, transforming growth factor-β (TGF-β), and IGF-1 were detected in lower concentrations with the use of Fibrinet. In contrast, the Regen displayed high concentrations of TGF-β, basic fibroblast growth factor, and IGF-1, whereas the Plateltex showed a high level of epidermal growth factor [43].

SVF can favor neoangiogenic vascularization and fibrogenic activity of fibroblasts that favor adipose tissue survival and three-dimensional organization. Compared with traditional fat grafting, the survival of the graft is more probable and fat necrosis is reduced, potentially because of improved vascular development in the implanted area. Results of this study offer an in vivo tissue-engineering approach that provides an optimized microenvironment, supporting the correct architectural adipocyte distribution, better cell-to-cell interaction, adipose tissue survival, and maybe limited differentiation from SVF; this could offer early protection from surrounding inflammatory events. Also, the early establishment of new microcapillary networks, which deliver the proper nutrients and oxygen to the implant, might contribute to the improved outcomes observed [1, 44, 45]. In fact, in the adipose tissue, ASCs reside between adipocytes or in the extracellular matrix, especially around vessels, and contribute to the turnover of adipose tissue, which is known to be very slow (2 years or more) [46].

However, adipose grafts probably turn over during the first 2–3 months after transplantation because they experience temporary ischemia followed by reperfusion injury. This turnover, the replacement process of the adipose tissue, is conducted by tissue-specific progenitor cells, which are ASCs. The relative deficiency of ASCs in aspirated fat may affect the replacement process and lead to postoperative atrophy of grafted fat, which is known to occur commonly during the first 6 months after lipoinjection.

After transplantation, ASCs may interact with other cells, such as vascular endothelial cells, and supplementation with the SVF may be superior to supplementation with ASCs alone in this treatment. However, additional studies are needed to elucidate the synergistic effects of ASCs with other cells contained in the graft.

In this preliminary study, satisfactory clinical results were generally achieved without any major complications. Thus, we can conclude that SVF-enhanced fat graft is sufficiently safe for continuation of the study, although controlled investigations and accumulated long-term results are needed to elucidate the overall safety and efficacy of the treatment. A variety of innovations, including stem cell technology, may be developed and may contribute to the improvement of autologous tissue transplantation and regeneration. Further improvements of the technique may cause autologous tissue transfer to become the first choice for breast augmentation in the future.

Furthermore, the use of other types of scaffolds for breast reconstruction should be noted. Colwell et al. [47], in a retrospective review of 331 consecutive breast reconstructions with acellular dermal matrix, demonstrated that this matrix offers a cost-effective reconstruction with a low complication rate. In addition, a recent review showed that acellular dermal matrix in two-stage expander/implant reconstruction offers a safety profile similar to that of standard submuscular techniques [48]. Several studies have been published on the use of acellular matrix, showing both the advantages and disadvantage of this technique [49, 50]. We believe that this matrix may be the procedure of choice in select patients.

Conclusion

We conclude that engineered fat grafting based on the addiction of SVF or PRP is a reliable alternative to breast implant based on some initial indications. (a) A preliminary study with follow-up at 30 months showed with instrumental imaging the absence of calcification or microcalcification. (b) This absence suggests that engineered fat grafting is effective and safe. (c) Autologous fat tissue can be used as a scaffold. (d) PRP and SVF favor adipose tissue survival. Additional study is necessary to evaluate the efficacy of this method further.

Author Contributions

P.G.: conception and design, manuscript writing; C.D.P., I.B., C.B.C., and M.F.: data analysis and interpretation; M.G.S.: collection and assembly of data; A.O.: conception and design, provision of study material; V.F. and R.F.: instrumental imaging analysis; V.C.: administrative support, final approval of the manuscript.

Disclosure of Potential Conflicts of Interest

The authors indicate no potential conflicts of interest.

References

1 Rigotti G, Marchi A, Galie M et al. Clinical treatment of radiotherapy tissue damage by lipoaspirate transplant: A healing process mediated by adipose-derived adult stem cells. Plast Reconstr Surg 2007;119:1409–1422; discussion 1423–1404.

2 Yoshimura K, Sato K, Aoi N et al. Cell-assisted lipotransfer for cosmetic breast augmentation: Supportive use of adipose-derived stem/stromal cells. Aesthetic Plast Surg 2008; 32:48–55; discussion 56–47.

3 Rigotti G, Marchi A, Stringhini P et al. Determining the oncological risk of autologous lipoaspirate grafting for post-mastectomy breast reconstruction. Aesthetic Plast Surg 2010;34:475–480.

4 Yoshimura K, Asano Y, Aoi N et al. Progenitor-enriched adipose tissue transplantation as rescue for breast implant complications. Breast J 2010;16:169–175.

5 Lendeckel S, Jodicke A, Christophis P et al. Autologous stem cells (adipose) and fibrin glue used to treat widespread traumatic calvarial defects: Case report. J Craniomaxillofac Surg 2004;32:370–373.

6 García-Olmo D, Garcia-Arranz M, Herreros D et al. A phase I clinical trial of the treatment of Crohn's fistula by adipose mesenchymal stem cell transplantation. Dis Colon Rectum 2005;48:1416–1423.

7 García-Olmo D, Herreros D, De-La-Quintana P et al. Adipose-derived stem cells in Crohn's rectovaginal fistula. Case Report Med 2010;2010:961758.

8 Garcia-Olmo D, Herreros D, Pascual I et al. Expanded adipose-derived stem cells for the treatment of complex perianal fistula: A phase II clinical trial. Dis Colon Rectum 2009;52:79–86.

9 Garcia-Olmo D, Herreros D, Pascual M et al. Treatment of enterocutaneous fistula in Crohn's disease with adipose-derived stem cells: A comparison of protocols with and without cell expansion. Int J Colorectal Dis 2009;24: 27–30.

10 Peterson B, Zhang J, Iglesias R et al. Healing of critically sized femoral defects, using genetically modified mesenchymal stem cells from human adipose tissue. Tissue Eng 2005; 11:120–129.

11 Yoshimura K, Sato K, Aoi N et al. Cell-assisted lipotransfer for facial lipoatrophy: Efficacy of clinical use of adipose-derived stem cells. Dermatol Surg 2008;34:1178–1185.

12 Tiryaki T, Findikli N, Tiryaki D. Staged stem cell-enriched tissue (SET) injections for soft tissue augmentation in hostile recipient areas: A preliminary report. Aesthetic Plast Surg 2011;35:965–971.

13 Lo Cicero V, Montelatici E, Cantarella G et al. Do mesenchymal stem cells play a role in vocal fold graft survival? Cell Prolif 2008;41: 460–473.

14 Cantarella G, Mazzola RF, Domenichini E et al. Vocal fold augmentation by autologous fat injection with lipostructure procedure. Otolaryngol Head Neck Surg 2005;132: 239–243.

15 Oedayrajsingh-Varma MJ, van Ham SM, Knippenberg M et al. Adipose tissue-derived mesenchymal stem cell yield and growth characteristics are affected by the tissue-harvesting procedure. Cytotherapy 2006;8:166–177.

16 Prunet-Marcassus B, Cousin B, Caton D et al. From heterogeneity to plasticity in adipose tissues: Site-specific differences. Exp Cell Res 2006;312:727–736.

17 Gimble JM, Katz AJ, Bunnell BA. Adipose-derived stem cells for regenerative medicine. Circ Res 2007;100:1249–1260.

18 Coleman SR. Facial recontouring with lipostructure. Clin Plast Surg 1997;24:347–367.

19 Coleman SR. Long-term survival of fat transplants: Controlled demonstrations. Aesthetic Plast Surg 1995;19:421–425.

20 Cervelli V, Gentile P, Scioli MG et al. Application of platelet-rich plasma in plastic surgery: Clinical and in vitro evaluation. Tissue Eng Part C Methods 2009;15:625–634.

21 Cervelli V, Gentile P, Grimaldi M. Regenerative surgery: Use of fat grafting combined with platelet-rich plasma for chronic lower-extremity ulcers. Aesthetic Plast Surg 2009;33: 340–345.

22 Cervelli V, Gentile P. Use of cell fat mixed with platelet gel in progressive hemifacial atrophy. Aesthetic Plast Surg 2009;33:22–27.

23 Kevy SV, Jacobson MS. Comparison of methods for point of care preparation of autologous platelet gel. J Extra Corpor Technol 2004;36:28–35.

24 Siebrecht MA, De Rooij PP, Arm DM et al. Platelet concentrate increases bone ingrowth into porous hydroxyapatite. Orthopedics 2002; 25:169–172.

25 Waters JH, Roberts KC. Database review of possible factors influencing point-of-care platelet gel manufacture. J Extra Corpor Technol 2004;36:250.

26 Man D, Plosker H, Winland-Brown JE. The use of autologous platelet-rich plasma

(platelet gel) and autologous platelet-poor plasma (fibrin glue) in cosmetic surgery. Plast Reconstr Surg 2001;107:229.

27 Lozada JL, Caplanis N, Proussaefs P et al. Platelet-rich plasma application in sinus graft surgery: Part I. Background and processing techniques. J Oral Implantol 2001;27:38.

28 Hood AG, Arm DM. Topical application of autogenous tissue growth factors for augmentation of structural bone graft fusion. Paper presented at: American Society of Extra-Corporeal Technology 11th Annual Symposium on New Advances in Blood Management; April 20–23, 2004; Las Vegas, NV.

29 Salgarello M, Visconti G, Rusciani A. Breast fat grafting with platelet-rich plasma: A comparative clinical study and current state of the art. Plast Reconstr Surg 2011;127:2176–2185.

30 Cervelli V, Gentile P, De Angelis B et al. Application of enhanced stromal vascular fraction and fat grafting mixed with PRP in post-traumatic lower extremity ulcers. Stem Cell Res 2011;6:103–111.

31 Citri A, Yarden Y. EGF-ERBB signalling: Towards the systems level. Nat Rev Mol Cell Biol 2006;7:505–516.

32 Schneider MR, Wolf E. The epidermal growth factor receptor ligands at a glance. J Cell Physiol 2009;218:460–466.

33 Giacco F, Perruolo G, D'Agostino E et al. Thrombin-activated platelets induce proliferation of human skin fibroblasts by stimulating autocrine production of insulin-like growth factor-1. FASEB J 2006;20:2402–2404.

34 Petit JY, Lohsiriwat V, Clough KB et al. The oncologic outcome and immediate surgical complications of lipofilling in breast cancer patients: A multicenter study: Milan-Paris-Lyon experience of 646 lipofilling procedures. Plast Reconstr Surg 2011;128:341–346.

35 Pulagam SR, Poulton T, Mamounas EP Long-term clinical, radiologic results with autologous fat transplantation for breast augmentation: Case reports, review of the literature. Breast J 2006;12:63–65.

36 Kwak JY, Lee SH, Park HL et al. Sonographic findings in complications of cosmetic breast augmentation with autologous fat obtained by liposuction. J Clin Ultrasound 2004; 32:299–301.

37 Gutowski KA; ASPS Fat Graft Task Force. Current applications and safety of autologous fat grafts: A report of the ASPS fat graft task force. Plast Reconstr Surg. 2009;124:272–280.

38 Fraser JK, Hedrick MH, Cohen SR. Oncologic risks of autologous fat grafting to the breast. Aesthet Surg J 2011;31:68–75.

39 Nedelec B, Shankowsky HA, Tredget EE. Rating the resolving hypertrophic scar: Comparison of the Vancouver Scar Scale and scar volume. J Burn Care Rehabil 2000;21: 205–212.

40 Lin K, Matsubara Y, Masuda Y et al. Characterization of adipose tissue-derived cells isolated with the Celution system. Cytotherapy 2008;10:417–426.

41 Rehman J, Traktuev D, Li J et al. Secretion of angiogenic and antiapoptotic factors by human adipose stromal cells. Circulation 2004; 109:1292–1298.

42 Anitua E, Sánchez M, Nurden AT et al. Autologous fibrin matrices: A potential source of biological mediators that modulate tendon cell activities. J Biomed Mater Res A 2006;77: 285–293.

43 Mazzucco L, Balbo V, Cattana E et al. Not every PRP-gel is born equal. Evaluation of growth factor availability for tissues through four PRP-gel preparations: Fibrinet, RegenPRP-Kit, Plateltex and one manual procedure. Vox Sang 2009;97:110–118.

44 Cao Y, Sun Z, Liao L et al. Human adipose tissue-derived stem cells differentiate into endothelial cells in vitro and improve postnatal neovascularization in vivo. Biochem Biophys Res Commun 2005;332:370–379.

45 Zhu M, Zhou Z, Chen Y et al. Supplementation of fat grafts with adipose-derived regenerative cells improves long-term graft retention. Ann Plast Surg 2010;64:222–228.

46 Strawford A, Antelo F, Christiansen M et al. Adipose tissue triglyceride turnover, de novo lipogenesis, and cell proliferation in humans measured with 2H2O. Am J Physiol Endocrinol Metab 2004;286:E577–E588.

47 Colwell AS, Damjanovic B, Zahedi B et al. Retrospective review of 331 consecutive immediate single-stage implant reconstructions with acellular dermal matrix: Indications, complications, trends, and costs. Plast Reconstr Surg 2011;128:1170–1178.

48 Sbitany H, Serletti JM. Acellular dermis-assisted prosthetic breast reconstruction: A systematic and critical review of efficacy and associated morbidity. Plast Reconstr Surg 2011;128:1162–1169.

49 Kim JY, Davila AA, Persing S et al. A meta-analysis of human acellular dermis and submuscular tissue expander breast reconstruction. Plast Reconstr Surg 2012;129: 28–41.

50 Hoppe IC, Yueh JH, Wei CH et al. Complications following expander/implant breast reconstruction utilizing acellular dermal matrix: A systematic review and meta-analysis. Eplasty 2011;11:e40.

See www.StemCellsTM.com for supporting information available online.

A Comparative Translational Study: The Combined Use of Enhanced Stromal Vascular Fraction and Platelet-Rich Plasma Improves Fat Grafting Maintenance in Breast Reconstruction

Pietro Gentile, Augusto Orlandi, Maria Giovanna Scioli, Camilla Di Pasquali, Ilaria Bocchini, Cristiano Beniamino Curcio, Micol Floris, Valeria Fiaschetti, Roberto Floris and Valerio Cervell

Stem Cells Trans Med 2012;1;341-351; originally published online April 13, 2012;
DOI: 10.5966/sctm.2011-0065